ELSEVIER

Biophysical Chemistry 101–102 (2002) 611–623

Biophysical Chemistry

www.elsevier.com/locate/bpc

Atomic force microscopy reveals kinks in the p53 response element DNA

P. Balagurumoorthy[a,*], Stuart M. Lindsay[b], Rodney E. Harrington[a]

[a]*Department of Microbiology, Arizona State University, Tempe, AZ 85287, USA*
[b]*Department of Physics and Astronomy, Arizona State University, Tempe, AZ 85287, USA*

Received 12 December 2001; received in revised form 23 January 2002; accepted 23 January 2002

Abstract

p53 is a 53 kDa nuclear phosphoprotein. Its function as a tumor suppressor critically lies in its ability to recognize its target DNA response elements as a tetramer. Here, we report the structural theme intrinsic to the response element DNA that governs this recognition phenomenon. The intrinsic flexibility or dynamic bending between two distinctly different, but naturally occurring p53 response elements has been compared by ring closure. Results show that DNA binding sites containing helically phased d(CATG.CATG) tetra-nucleotide sequences at the centers of *quasi*-dyad symmetry in each half-response site are more *intrinsically* flexible (i.e. preferentially bent under axial stress) than their d(CTTG.CTTG) counterparts. Intriguingly, p53 binding sites containing these more flexible d(CATG.CATG) sequence elements also exhibit a stronger tendency for tetrameric binding of the p53 DNA binding domain peptide. Examination of the shapes of DNA microcircles obtained by circularization of oligomers constructed from such flexible p53 target DNA sequences in tandem using MacMode atomic force microscopy directly revealed sequence-specific kinks in solution. The tetra-nucleotide sequence d(CATG.CATG) is highly conserved in most functional p53 response elements. Consequently, we propose that the sequence-specific kinks originating from d(CATG.CATG) sequences could be a common structural theme in p53 response elements and as evident from the results reported here, could be a determinant of binding site recognition by the p53 protein and the subsequent stability of the p53–DNA complex.

Keywords: p53; $p21^{waf1}$ response element; MacMode atomic force microscopy; Kink; Contour length; DNA flexibility

1. Introduction

p53 is a 53 kDa nuclear phosphoprotein that occurs in a wide variety of organisms. It plays a key role in tumor suppression [1–4]. Its inactivation, either through mutations or by its association with other viral or cellular proteins, is common in the onset of most human cancers [5]. p53 is the central player in the pathways controlling cell growth, DNA repair, differentiation and programmed cell death [1,4]. Wild type p53 functions as a transcription factor in response to DNA damage [1,6,7]. It activates genes such as *waf1*,

*Corresponding author. Tel.: +1-480-965-0177; fax: +1-480-965-0098.
E-mail address: balaguru@asu.edu (P. Balagurumoorthy).

0301-4622/02/$ - see front matter © 2002 Elsevier Science B.V. All rights reserved.
PII: S0301-4622(02)00169-2

gadd45, *cyclin G*, *mdm2*, *bax*, 14-3-3σ, FAS/APO1, KILLER DR5, PIG3, Tsp1 and IGF-BP3 whose gene products interfere with global cellular events such as growth, arrest, and cell death or apoptosis [7]. There are more than 100 functional p53 binding sites in the human genome [8,9] located either upstream of the 5′-UTR as in $p21^{waf1}$ [6,7] or in the intronic gene promoters as in the *mdm2* gene [10,11]. The ability of p53 to bind sequence-specifically to such DNA response elements is critical to its function [9,12]. Wild-type p53 consists of three major functional domains [1], the C-terminal tetramerization domain, the N-terminal transactivation domain and the central DNA binding domain (p53DBD) encompassing amino acid residues from 96 to 208. In more than half of human cancers, a direct inactivation of p53 through point mutations has been reported [13]. Many of the tumorigenic point mutations are mapped to its central DNA binding domain [14] and result in the complete or partial loss of its DNA binding activity [1]. Therefore, it is becoming increasingly important to understand the structural principles underlying this recognition event.

Most of the p53 response elements consist of two contiguous decameric half sites. The half sites fall into a subset consensus RRRCA/t|T/aGYYY, in which the pentameric 'quarter sites' are separated by a *pseudodyad* symmetry indicated by a vertical bar [8,9]. Several studies have shown that wild type p53 binds to its 20 bp response element DNA, predominantly as a tetramer [15] with each molecule of p53 making specific contacts with a pentameric quarter site [16,17]. A co-crystal structure of a single DNA binding domain of wild-type p53 (p53DBD) specifically bound to a pentameric 'quarter site' embedded in a DNA fragment, provided significant insights into the protein–DNA contacts critical for recognition [14]. This high-resolution structure revealed a high incidence of direct correlation between amino acid residues critically involved in the protein–DNA contacts and their mutation frequency in human cancers. However, the exact nature of the interactions between the tetrameric p53 bound to a full 20 bp target DNA site could not be precisely extrapolated from this high-resolution crystal structure.

Studies from this laboratory showed that the DNA binding domain of wild type p53 (p53DBD) itself is capable of assembling as a tetramer on its target DNA response elements in the absence of the tetramerization domain [16,17]. Recent AFM studies from this laboratory showed that the existence of p53 as a preformed tetramer in solution enhances the binding specificity of p53 to its target DNA several fold as compared to p53DBD (Balagurumoorthy et al., unpublished results). In either case, with or without the tetramerization domain, p53 binding to the target DNA was accompanied by substantial bending and twisting of the response element DNA [16–19]. Detailed molecular modeling and energy minimization studies [20] corroborated the conclusions drawn on the bending and twisting detected in the p53–DNA complexes from cyclization [16], phasing analysis [19] and atomic force microscopy [21] (Balagurumoorthy et al., unpublished results). The molecular modeling studies suggested that the DNA bending/twisting relieves steric clashes between adjacently bound p53 moieties in the tetrameric p53–DNA complex [20,22]. These studies also suggested that such bending occurs through kinking at the unique flexible sites found at the *pseudo-dyad* junction between the two pentameric quarter sites [16,17,20] and in addition, *over*-twisting of the DNA by p53 was shown to act synergistically with DNA bending in stabilizing the p53 tetramer–DNA complex [19,20]. Recently, using MacMode AFM in solution, we showed that such over-twisting could be intrinsic to the p53 response element DNA itself [21].

In this paper, we present direct experimental evidence for the kinks resulting from the anisotropically flexible d(CATG.CATG) sequences in the $p21^{waf1}$ p53 response element. These results are consistent with the ability of such sequences to roll either into a major or minor groove that emerged from molecular modeling studies [20], which to date provide the only available structural model for the tetrameric p53–DNA complex. The experiments described here, address a number of important questions concerning the importance of sequence-dependent DNA structure in p53 binding specificity. These results, when combined with other studies which demonstrate correlation

5′tccgaT**GAACATGTCC***ATGAATTAAT***CAACATGTTG**ggcctt 3′ **WAFS**

3′ ta**CTTGTACAGG***TACTTAATTA***GTTGTACAAC**ccggaaaggc 5′

5′tccgat**TGCCTTGCCT***ATGAATTAAT***GGACTTGCCT**ggcctt 3′ **RGCS**

3′ ta**ACGGAACGGA***TACTTAATTA***CCTGAACGGA**ccggaaaggc 5′

Fig. 1. Precursor oligonucleotide duplexes used in this study. $p21^{waf1}$ and RGC response elements were incorporated into 42 bp oligonucleotide sequences (exactly four helical turns) WAFS and RGCS, respectively, with a helical turn (10 bp) of spacer DNA between the decameric half sites, indicated in bold. The flanking sequences are shown in lower case and the spacer DNA is indicated in italics. Cohesive ends that are four bases long in WAFS and RGCS ensure efficient head-to-tail ligation of precursor units to form microcircles.

between these critical sequences and p53 binding affinity [22], suggest that the intrinsic DNA flexibility inherent and critically positioned in the p53 binding half sites is important to specific tetrameric binding of p53 to its DNA response elements, and may serve as a structural means by which the various p53 response elements are differentiated from each other in their biological functions. With a view towards the many recently discovered chromatin remodeling factors, we speculate that such sequence-specific structural microheterogeneity and distortion in the DNA sequences in chromatin supramolecular assemblies might be recognized by transcription factors such as p53.

2. Experimental

2.1. Expression and purification of the p53DBD

The PCR amplified region of human p53 cDNA encoding amino acids from 96 to 308 was cloned in a pET12a expression vector (Novagen) and transformed into an *Escherichia coli* BL21 (DE3) strain. The cells were grown at 37 °C until they reached an OD_{600} of 0.6–1.00. Then, isopropyl-β-D-thiogalactoside (IPTG) was added to a final concentration of 0.25 mM to induce the expression of p53DBD. After 2 h of induction, the cells were lysed in a French press and sonicated for 2 min in 40 mM Mes-Na, pH 6.8, 100 mM NaCl/5 mM DTT. The soluble fraction was loaded onto a Resource S (Pharmacia) column in 40 mM Mes-Na, pH 6.8/5 mM DTT, and was eluted by a 0–400 mM NaCl gradient. The fractions containing p53DBD were pooled together and precipitated by adding ammonium sulfate to 80% saturation. The precipitated protein was further purified on a Superdex 75 HR gel filtration (Pharmacia) column in 50 mM bis-Tris propane–HCl, pH 6.8, 100 mM NaCl/1 mM DTT. The purified p53DBD ran as a single band on an SDS-polyacrylamide gel [16].

2.2. Electrophoretic mobility shift assay

The qualitative determination of the binding affinity of p53DBD to the oligonucleotide probes WAFS and RGCS shown in Fig. 1, were carried out as previously described [16]. Ten nanograms of 5′ end-labeled DNA probe was incubated on ice for 40 min with varying concentrations of p53DBD in 10 μl of 50 mM bis-Tris propane–HCl, pH 6.8, 100 mM NaCl, 1 mM DTT and 100 ng of poly (dI–dC). Two microliters of 30% glycerol was added to the binding reaction and the samples were analyzed on a 5% non-denaturing polyacrylamide gel in 0.3X TBE.

2.3. DNA cyclization or ring closure

DNA flexibility and bending in the p53 binding sequences WAFS and RGCS were quantified by

T4 ligase mediated cyclization as described previously [16]. The microcircles from the second-dimensional chloroquine gels were eluted out, and their sizes were determined on a denaturing polyacrylamide gel with the ligation ladder of the same oligonucleotide and Msp I digest of pBR322 DNA as size markers. The microcircles of 168 bp (4×42 bp) were pooled together from several gels and passed through a NAP10 (Pharmacia) column equilibrated with water. Microcircles were dissolved in 0.1 mM Tris–HCl, pH 8.0 at a concentration of 0.5 μg/ml and stored at −20 °C.

2.4. Mica modification and AFM imaging

3-Aminopropyltriethoxysilane (APTES) (98%; Sigma Chemical Co., St. Louis, MO, USA) was distilled once under vacuum prior to use. One part of this reagent was mixed with 10 000 parts of water. Ten microliters of this suspension was placed on a freshly cleaved mica and washed away after 5 min with 200 μl of water. Then, the mica surface was blown dry with argon. Three hundred microliters of solution containing DNA microcircles (0.5 μg/ml) in 0.1 mM Tris–HCl, pH 8 was added onto the mica clamped with AFM liquid cell and imaged under the Tris buffer after 15 min.

The AFM imaging was carried out using a PicoSPM from Molecular Imaging (Phoenix, AZ, USA). This instrument utilizes a top-down scanner with a lightweight sample plate suspended below it magnetically. The liquid cell is a one-piece Teflon well, which clips onto the mica on the sample plate. Images were collected with a magnetic AC drive (MacMode) using silicon cantilevers of nominal spring constant 0.6 N/m. The drive frequency was 25 kHz. The free operating amplitude was set at 5 nm p/p with a 10% reduction set point. The instrument was calibrated at regular intervals using a 1-μm^2 grating from Silicon MDT, Moscow, Russia and checked by measuring the contour length of pUC19 DNA.

2.5. Analysis of the AFM images

The x–y coordinates of the microcircles were extracted from AFM images using NIH Image software. These coordinates were scatter-plotted in two dimensions using Kaleidagraph software and these plots were aligned on the top of each other using Adobe Photoshop (version 5.1). The distances between the kinks were measured using NIH Image software using the experimentally observed average contour length as the perimeter of the averaged x–y scatter plot.

3. Results and discussion

3.1. Sequence-dependent DNA binding specificity of tetrameric p53DBD

It is known that wild type p53 binds to DNA response elements in which the decameric half sites are separated by a spacer DNA of length varying from 0 to 21 bp [8,9,23,24]. Such p53 response elements occur naturally in the human genome and have been shown to be functional in a few cases [23]. We have used two functionally important p53 response elements, $p21^{waf1}$ and RGC, with 10 bp of spacer inserted between the half sites. Using this as a model system, we demonstrate the influence of DNA flexibility on the binding specificity of p53DBD. Two 42 bp oligonucleotides (WAFS and RGCS) used in this study are shown in Fig. 1. The first of these has a d(CATG.CATG) sequence at the pentameric pseudodyad junctions in the half sites, whereas the second has d(CTTG.CTTG). These two tetranucleotide sequences are representative of two extreme degrees of anisotropic flexibility on the basis of their ability to roll into either major or minor grooves [25–27].

The gel mobility shift assay used to determine the binding ability of p53DBD to these sequences is shown in Fig. 2. WAFS exhibits two shifted bands rb1 and rb2 at the lower p53DBD concentrations of 0.042 and 0.209 nM. A further increase in the p53DBD concentration to 1.05 nM, resulted in the complete shift of the entire labeled DNA to rb2, accompanied by the complete disappearance of rb1. These observations suggest that the band rb2 corresponds to the tetrameric p53DBD–DNA complex and rb1 a dimer bound to the DNA. The tetrameric binding of p53DBD to WAFS takes place in two stages in a non-cooperative manner in contrast to the cooperative binding observed for

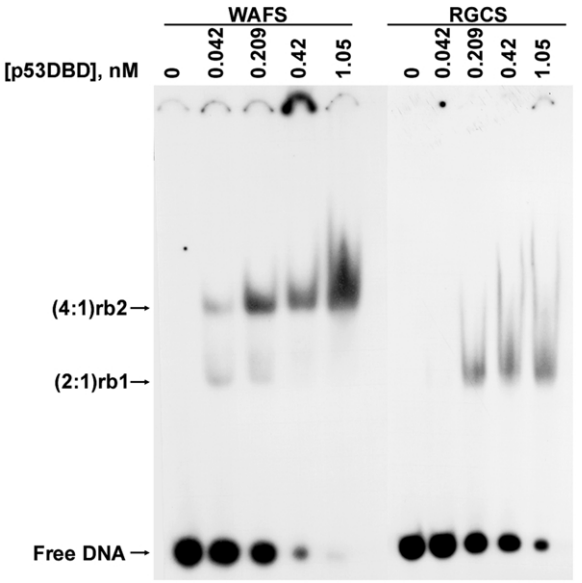

Fig. 2. Electrophoretic mobility shift assays used to qualitatively determine the difference in binding affinity between WAFS and RGCS to p53DBD. A fixed amount (10 ng) of a 5′ end-labeled oligonucleotide duplex probe was titrated with increasing concentrations of p53DBD, as indicated on the top. The resulting p53DBD–DNA complexes were analyzed on a 5% non-denaturing polyacrylamide gel, along with the same amount of unbound/free DNA as a control.

the unspaced *waf1* response element [16]. However, from lane 4, it can be noted that WAFS binds tetrameric p53DBD at or above 0.42 nM p53DBD. Interestingly, this is not the case with RGCS, which exhibits only one shifted band even at 1.05 nM p53DBD. The mobility of this shifted band matches with that of rb1, indicating that RGCS only binds a dimer of p53DBD. The inability of RGCS to bind a tetrameric p53DBD is evidenced by the absence of a shifted band, whose mobility would match with the retarded band rb2. Furthermore, when the spacer DNA was replaced by a GC rich DNA sequence in WAFS and RGCS, the protein binding properties to these spaced response elements remained unaltered (Balagurumoorthy et al., unpublished). Therefore, this remarkable difference in the protein binding ability between WAFS and RGCS suggests that the presence of d(CATG.CATG) in the half sites is required for tetrameric binding of p53DBD to the 'split' response elements.

These observations are consistent with the results reported by Miner and Kulesz-Martin [23] in which it was shown that tetrameric p53 binding to response elements with a spacer DNA up to 23 bp in length, occurs preferentially to half sites containing d(CATG.CATG). Thus, we wanted to understand these differences in p53 binding preference, since earlier studies from this laboratory [16,19,22] and elsewhere [18] on unspaced p53 response elements, showed that bending of the DNA helical axis in the p53–DNA complex is required for nucleoprotein complex formation and stability. We had speculated earlier [16,19,20] that such DNA bending could promote favorable protein–protein contacts between bound dimers on either side of the spacer DNA and hence, would be necessary for complex stability.

The sequence element d(CA·TG) is known to possess unusual anisotropic flexibility and has a propensity to kink into either the major or minor grooves [25–28]. Several nucleoprotein complexes are known to exhibit kinking at d(CA·TG) dinucleotide steps [29–34]. In the context of the results reported here, it is worthwhile mentioning that the X-ray crystal structure of the oligonucleotide d(AGGCATGCCT·AGGCATGCCT), which falls under the subset consensus RRRCA/TT/AGYYY defined for p53 binding half sites, displayed a large roll angle towards the minor groove at the d(CA·TG) steps, resulting in a non-linear helical axis [35]. Using ring closure methods [36], Lyubchenko et al. showed that the λ phage *Cro* protein complexed with its OR3 binding site is bent by 45° [31], with the putative assignment of the bending locus to the flexible d(CA·TG) dinucleotide step. The results from ring closure experiments have been corroborated by X-ray crystallography [37] and scanning force microscopy [38], and the magnitudes of DNA bending obtained from these different methods are in relatively good agreement with each other. The DNA cyclization experiments are carried out entirely in solution and are well understood theoretically, in contrast to other gel mobility based techniques. Therefore, we opted for a T4 DNA ligase mediated ring closure method to investigate whether there may be an unusual struc-

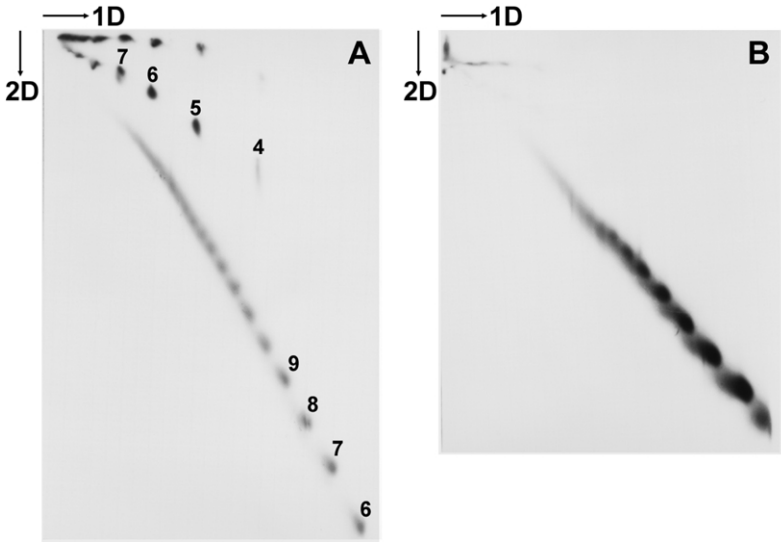

Fig. 3. Second dimensional polyacrylamide gels used to quantitate the intrinsic flexibility/bending in the 42-mers WAFS (a) and RGCS (b) containing $p21^{waf1}$ and RGC response elements, respectively. 1D, first dimension (5%) and 2D, second dimension (8%). The central row of spots represent covalently closed microcircles and the nicked microcircles of the corresponding sizes appear above this. The bottom diagonal consists of linear ligamers. A second dimension was run in the presence of 50 μg/ml of chloroquine to enable the separation of linear ligamers from the covalently closed and nicked microcircles. The sizes of the microcircles and linear ligamers are indicated in terms of the number of basic precursor units (e.g. 4 represents $4\times42=168$ bp).

tural property associated with the d(CATG·CATG) containing p53 binding sites, that can account for the observed difference in p53-tetrameric binding specificity between the WAFS and RGCS response elements.

3.2. DNA flexibility in WAFS and RGCS

Fig. 3 shows the second dimension chloroquine–polyacrylamide gels for WAFS (a) and RGCS (b). Cyclization reactions on these 42-mers containing $p21^{waf1}$ and RGC p53 response elements were carried out in the absence of p53DBD. In Fig. 3a, the second row of spots from the top represent covalently closed microcircles. These microcircles retain the topology and writhe introduced due to the sequence-dependent DNA structural deformations intrinsic to the $p21^{waf1}$ response element in the precursor unit WAFS during the ring closure by T4 DNA ligase. Corresponding sized nicked microcircles appear above these. The linear ligamers lie on the bottom diagonal. The adjacent spots or bands differ from each other by a single precursor unit of 42 bp. It is apparent from the spot intensities that WAFS circularizes well without p53DBD and microcircles as small as 168 bp (4×42 bp) made up of four precursor 42-mers can be detected. The microcircles of 168 bp and 210 bp are well below the size range expected due to thermal cyclization [33].

These observations suggest that the p53 binding half sites in WAFS are intrinsically flexible or dynamically bent. Fig. 3b shows the result of the same experiment carried out for RGCS under identical conditions. Intriguingly, ligation of RGCS did not yield a comparable amount of microcircles detectable under identical conditions. This indicates that RGCS containing d(CTTG·CTTG) in the p53 binding half sites is not intrinsically flexible. It is evident from the above experiments that the presence of d(CATG·CATG) at the pentamer junctions in the half sites imparts intrinsic flexibility to the response element DNA. This could account for the enhanced ability of p53 response elements with such flexible half sites to bind the p53DBD tetramer as shown in Fig. 2.

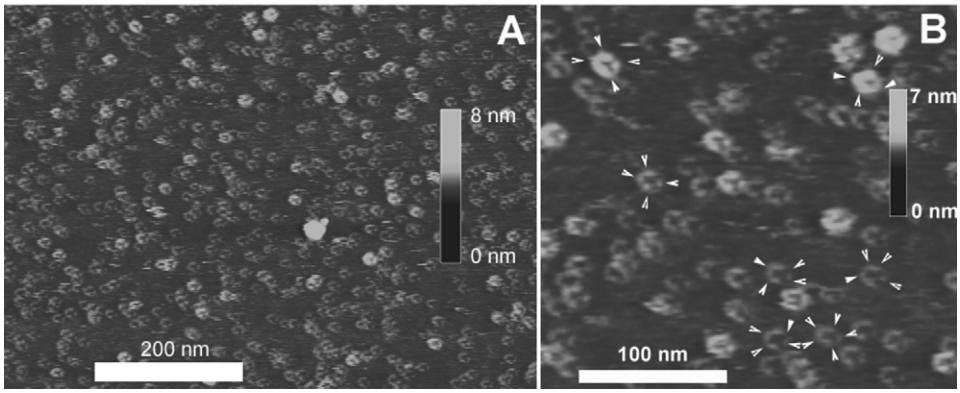

Fig. 4. MacMode AFM images of microcircles made up of four head-to-tail ligamers of WAFS containing four p21^{waf1} p53 response elements. The *x*–*y* scale is shown by a horizontal white bar and the vertical bar indicates the height. (A) image field obtained on a larger scan area on AP-mica in 0.1 mM Tris–HCl (pH 8.0). (B) High-resolution image showing the finer structure of the microcircles obtained by scanning a smaller area selected from (A). In (B), the kinks on the DNA microcircles are indicated by white arrow heads. Pairs of kinks are visible on the highest and lowest sides facing each other, in the microcircles with chair-like conformation.

Thus, there exists a direct correlation between the ability of WAFS to bind tetrameric p53 and its intrinsic flexibility. This interpretation is further supported by computer modeling of the DNA trajectory [39]. The ends of a linear DNA sequence with four WAFS precursor units in tandem come close enough to readily form microcircles only if a positive or a negative roll angle of 15–30° is allowed at each of the d(CA)·d(TG) dinucleotide steps. The resulting curved DNA trajectory appears to have hinges (kinks) wherever such a roll angle was permitted (Balagurumoorthy et al., unpublished results).

3.3. Periodically spaced kinks in p21^{waf1} microcircular DNA

Fig. 4 shows the MacMode AFM [40] images of the 168 bp microcircles derived from WAFS, obtained in 0.1 mM Tris–HCl, pH 8.0. We intentionally did not include any mono or divalent metal ions in the buffer, as alkaline earth and transition metal ions are known to alter the structure of the DNA adhered to a surface [41]. As can be seen in Fig. 4a, the overall structure of the microcircles is remarkably uniform throughout the scan area. The DNA trajectory in these microcircles is not smooth but rather shows regular, periodic kinking, unlike the random kinks observed for microcircles containing statically bent alternating A-tract/GGGCCC sequences [41]. Fig. 4b shows a high resolution scan of a small area from Fig. 4a. It is apparent that the majority of the present circles have four corners, implicating four visible kinks, indicated by arrowheads in Fig. 4b. The discontinuity visible in the DNA contour suggests that, unlike the alternating A-tract/GGGCCC sequences reported earlier which were clearly topologically flat, these microcircles containing p21^{waf1} binding sites are not perfectly planar but are puckered. The puckered circles adopt a chair-like conformation with one highest side opposite to the lowest side, and two arms of intermediate elevations between these positions facing each other. The fact that these two arms are not in a single plane led to the identification of two equally populated topoisomers with slightly different magnitudes of positive and negative writhe. On the basis of these structural features, we performed calculations to quantify the absolute twist in WAFS [21]. Consistent with the armchair-like topology of these microcircles [21], two kinks are observed on the highest side, opposite to the other two kinks located on the lowest side with the arms of intermediate elevations connecting these two sides in Fig. 4b.

The images obtained with the above characteristics were quite stable from scan to scan and reproducibly much broader at certain points along the contour. This effect could be accounted for by the finite radius of the imaging tip, if the broader points were also the highest points, and this is clearly the case as seen in the images. Nonetheless, the overall shape and the sharp kinks indicated by arrowheads cannot be a tip or surface-induced artifact because the orientation of the finer features varies within a single scan, though there seems to be a preferred orientation. However, since the contour including the inner rim of the microcircles are clearly revealed in the images of individual microcircles, we rule out any artifact due to tip-convolution effects.

The visible features of these images are highly reproducible over many preparations and many imaging sessions, and did not seem to depend on either the tip–surface interaction or subtle details of the sample deposition procedure. In this connection, we developed a new procedure to loosely adhere the DNA microcircles onto AP-treated mica, which is quite different from that usually done in tapping mode-air AFM imaging of soft biological samples [42]. This method eliminates the drying and hence, the possible dehydration of the substrate DNA after deposition on mica and hence, maintains solution conditions for the sample throughout the deposition process. In the present studies, the DNA solution at 0.5 μg/ml concentration was placed directly onto the AP-mica with no further treatment and imaged under the liquid. Thus, it is unlikely that adhesion of the microcircles to the surface alters the essential conformational features they would have in solution prior to deposition.

The 168 bp microcircles contain four p53 tetrameric full sites, derived from four precursor 42-mer units; each of these in turn, has two d(CATG·CATG) stretches separated by 20 bp. The adjacent pair of anisotropically flexible d(CATG·CATG) sites are separated from each other by 24 and 26 bp in an alternating fashion over the 168 bp microcircle, depending on whether they are derived from the same precursor unit or not. However, we would expect these microcircles to exhibit eight kinks if d(CATG·CATG) is the sole origin of their unusual flexibility. Since these circles are puckered rather than planar, we expected that kinks could also lie below the plane of the contours visible in the images shown in Fig. 4a,b. The discontinuities seen in the contours support this idea. Alternatively, the energetic cost of kinking four d(CATG.CATG) sites by 90° will be much lower than that of kinking eight flexible sites by 45° as suggested by calculations by Zhurkin et al. [25]. In this case, four properly phased kinks might be sufficient to allow ring closure. In any event, a more sophisticated analysis is required to locate the positions of these four major kinks on the 168 bp microcircles.

3.4. Locus of kinks in the p21^{waf1} response element

In order to localize the kinks to specific sites on the microcircle containing the p21^{waf1} response element, we have extracted the *x*- and *y*-coordinates along the contour circumferences of 125 individual microcircles from Fig. 4a and similar image fields, and have reconstructed their three-dimensional DNA trajectories. The shapes of these two-dimensional projections on a *x*–*y* plane are similar and all of them exhibit approximately a rectangular shape, with four major kinks and two minor kinks at the center. A few of these *x*–*y* scatter plots are shown in Fig. 5a. The 125 individual *x*–*y* plots are aligned on the top of each other to get an average statistical (scatter plot) picture of the microcircle conformation, and the result is shown in Fig. 5b. The thick arrows numbered 1, 2, 3 and 4 represent the positions of four kinks observed in the AFM images shown in Fig. 4b. Thin arrows indicate the positions of minor kinks that could lie below the plane connecting the major kinks 1, 2, 3 and 4 and hence, could be one of the dyad symmetry axes of the microcircle structure. The mean contour length of these 168 bp microcircles was found to be 57 nm, as measured directly from the images shown in Fig. 4b. Using this as a perimeter of the statistically averaged *x*–*y* plot, the distances between the kinks along the rim are measured and indicated in Fig. 5b. From these distances the exact separation between these kinks in base pairs is calculated. The separation between kinks 1 and 4, or 2 and 3

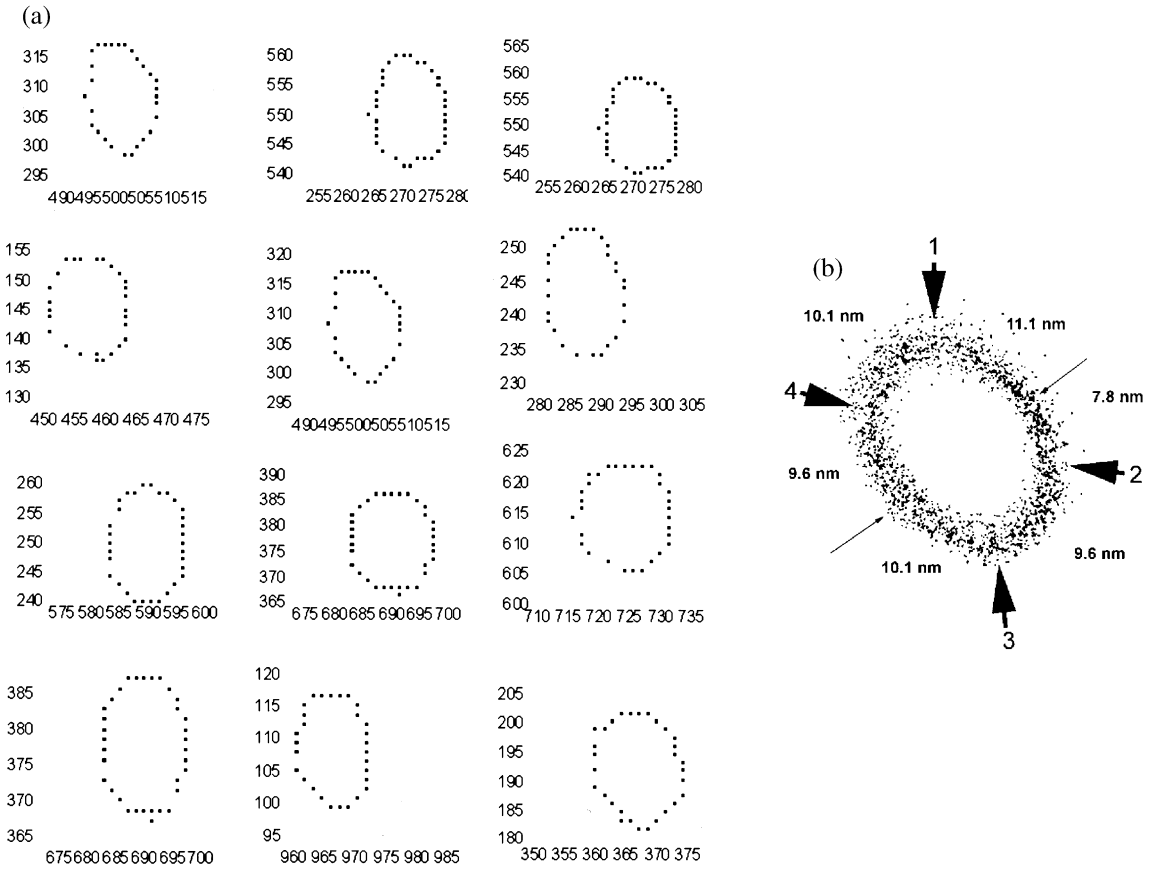

Fig. 5. (a) Representative x–y scatter plots of the contours of individual microcircles. The x- and y-axis are in nanometers and the points represent the (x, y) coordinates at selected places on the contour of a DNA microcircle, measured directly from an image field using NIH Image software. (b) Statistical average contour of 125 individual microcircles. The x–y coordinates were extracted from microcircles and scatter plotted as shown in (a). These two-dimensional projections of the DNA trajectory were superimposed on each other and aligned by free transformation. The individual contours could be aligned in only one particular orientation, in order to augment the additive effect of the kinks found in the individual contours. The resulting average contour of the microcircles was calibrated using the experimentally observed contour length of 57 nm and the distance between the kinks was measured. The four major kinks were numbered 1, 2, 3 and 4 and indicated by solid arrowheads. Thin arrows represent one of the several dyad symmetry axis and could be the out-of-plane positions along the molecular contour [21]. The separation between kinks 1, 4 and 2, 3 corresponds to 28 bp, which is in reasonable agreement with the actual 24 bp spanning the region over the neighboring d(CATG●CATG) stretches in a precursor unit.

turns out to be 28 bp. It can be noted from Fig. 1 that in the WAFS, the number of base pairs spanning the region from the CATG in the first half site to the CATG stretch in the next half site equals 24 bp. Thus, the agreement between the actual separation (24) and experimental separation obtained from the above image analysis (28 bp) is remarkably good considering the present resolution limits of solution-based atomic force microscopy under conditions of minimal tip-induced stresses. We can interpret these results as follows with reference to Fig. 5b. On the basis of the analysis (Fig. 5b), the two possible isomers of 168 bp $p21^{waf1}$ microcircles consistent with the experimentally-derived distances between the kinks, are schematically shown in Fig. 6. In the first possibility (Fig. 6a), kinks 1 and 4, and 2 and 3 are assigned to the pairs of successive

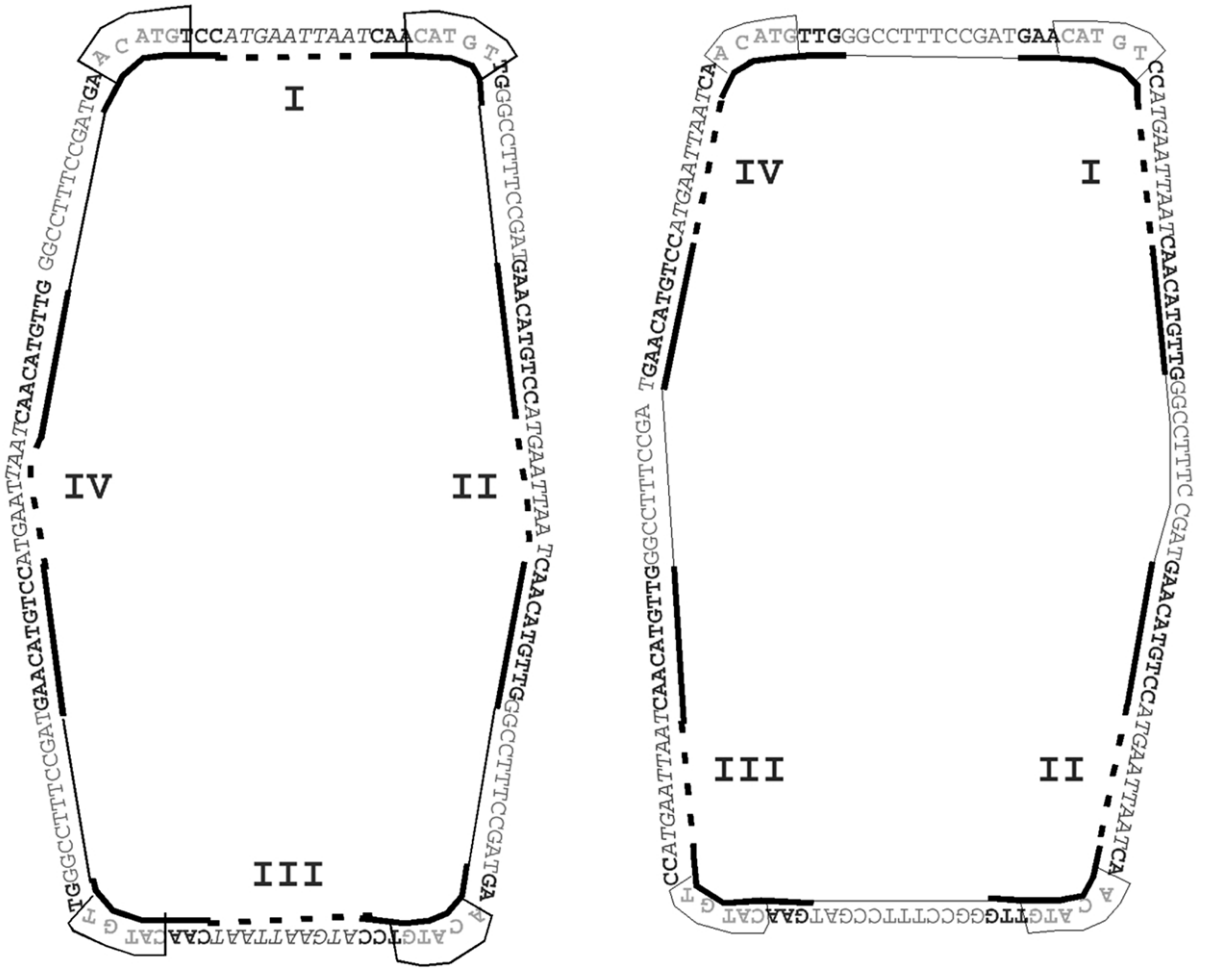

Fig. 6. Schematic diagram displaying the DNA sequence and conformation of the 168 bp p21^{waf1} microcircle. Two possible kinked isomers consisting of a 168 bp microcircle, consistent with the distance constraints obtained in Fig. 5b. The spacer DNA between the 10 bp half sites is indicated by a heavy dashed line and the flanking sequences shown in gray color by a thin solid line. In half sites that are shown in bold indicated by a heavy solid line, the DNA sequence spanning, the loci of the kinks are shown in boxes at the corners of the microcircle. The following assignments of the kinks to the specific sites in the microcircle are based on the distance constraints (Fig. 5b), in conjunction with the differences between WAFS and RGCS in their p53DBD binding properties (Fig. 2) and circularization efficiencies (Fig. 3). (a) The kinks were assigned to pairs of adjacent d(CATG·CATG) stretches, in alternating precursor units. The separation between the nearest kinks in this isomer is 24 bp. (b) Each precursor unit has a kink either in its first or second half site. Alternating half sites are kinked in a cyclic fashion. The number of basepairs separating the nearest kinks is 26, and is closer to the experimentally derived separation of 28 bp from Fig. 5b.

CATG sequences present in *alternating* 42-mer precursor units in the microcircles comprised of four such precursor units. In other words, if the precursor units in the 168 bp microcircle are numbered I–IV arbitrarily, two neighboring d(CATG·CATG) stretches either in units I and III, or II and IV are kinked at any given time. Alternatively, as depicted in Fig. 6b, each precursor unit could harbor a kink and alternating half sites are kinked in a cyclic fashion. In this second possible isomer, if the first half site is kinked in precursor unit I, then the second half site has to

be kinked in the next precursor unit II and vice versa, in order to accommodate the distance constraints shown in Fig. 5b. The separation between the nearest neighboring kinks is 24 and 26 bp in the isomers shown in Fig. 6a,b, respectively. The isomer shown in Fig. 6b is more likely to exist than that shown in Fig. 6a due to the fact that in this isomer each precursor unit has a kink, and the separation between the kinks (26 bp) is closer to the experimentally-derived distances between the kinks. Thus, the above analysis of images leads directly to the assignment of the four experimentally observed kinks to the tetranucleotide d(CATG·CATG) sequences in the 168 bp $p21^{waf1}$ microcircle.

4. Conclusions

The present studies directly implicate for the first time the direct involvement of specific flexible DNA sequence elements in the recognition of target DNA by p53. Although p53 response elements are diverse in their sequence, d(CATG·CATG) is highly conserved at the *pseudodyad* junctions in the majority of p53 binding decameric half sites [8,9]. A comprehensive molecular model proposed for the tetrameric p53–DNA complex required the response element DNA to bend in order to avoid steric clashes between the adjacently bound p53 molecules [20]. To achieve this, it was found to be energetically less expensive to kink the DNA at d(CATG·CATG) steps, as found in many other nucleoprotein complexes [30,32,37]. DNA flexibility and kinks observed in the $p21^{waf1}$ response element as reported here, provide a direct experimental evidence for the rationale used in the molecular modeling for a tetrameric p53DBD–DNA complex in the absence of a detailed X-ray crystal structure.

The *x*- and *y*-coordinates of 125 microcircles were obtained directly from the MacMode AFM image files, and were scatter plotted and superimposed on each other. It was found that the individual contours could be superimposed on each other only in one particular orientation, due to periodically spaced kinks. Although there is no marker on these microcircles, the present analysis confirms that the kinks originate from the d(CATG·CATG) tetranucleotide sequences in the $p21^{waf1}$ response element DNA as proposed in the original molecular model [17,20].

More fundamentally, in addition to stabilizing the nucleoprotein complex, kinks play a role in the recognition of response elements by p53, as suggested by the enhanced ability of WAFS to bind tetrameric p53DBD as compared to unkinked RGCS. It has recently been shown that p53 binds to nucleosomal DNA [43], but it is likely that some of the many naturally occurring p53 response elements are excluded from nucleosome formation, and differences in response element flexibility such as those noted here may play a role in this. Alternatively, chromatin remodeling factors and architectural proteins [44–46] such as SWI/SNF, may loosen the association between histones and nucleosomal DNA and create a free DNA bubble on the nucleosome by local DNA exclusion in the region of a p53 binding site. This could in turn, permit structural properties of the response element DNA such as flexibility and kinks to be recognized by p53, and could play a direct role in the specific binding of p53 to the response element. In the present work, we have shown that one of the several biologically important p53 response elements is kinked. This element is typical of many others in having specifically positioned flexibility sites. Given the sequence diversity of p53 binding sites and the functional diversity of the protein, it is likely that these positioned sites play an important role in the selectivity of binding to its various response elements that this remarkable protein shows. For example, architectural proteins such as HMG1 bind and bend the DNA in a non-sequence specific manner [47–49]. HMG1 has also been shown to increase the ability of p53 to bind its response element DNA and transactivate a target gene [50]. It is possible that HMG1 and other architectural proteins, in the context of a large transcriptional complex, could bend/kink p53 response element DNAs having less flexible sequences than d(CATG·CATG) at the response element *pseudodyads*, thus providing a pre-kinked conformation, similar to that of the $p21^{waf1}$ site reported here. This could provide an additional rationale for binding selectivity in p53 and its requirements for additional protein factors. All

these ideas are likely to be significant in understanding the multifaceted *in vivo* function of p53.

Acknowledgments

The authors gratefully acknowledge useful discussions, particularly with Dr Victor Zhurkin, Dr Ettore Appella and Dr Carol Prives. The authors thank Dr X.Z. Feng for help in MacMode AFM imaging and Dr Ilga Winicov and Dr Luda Shlyakhtenko for much useful information and support. Thanks are extended to Dr Ralph Bash and Mr Ken Eagan for useful discussions. Financial support is gratefully acknowledged from NIH grants GM53517 and CA70274 (REH).

References

[1] L.J. Ko, C. Prives, p53: puzzle and paradigm, Genes Dev. 10 (1996) 1054–1072.
[2] A.J. Levine, p53, the cellular gatekeeper for growth and division, Cell 88 (1997) 323–331.
[3] H.F. Ding, D.E. Fisher, Mechanisms of p53 mediated apoptosis, Crit. Rev. Oncog. 9 (1998) 83–98.
[4] B. Vogelstein, D. Lane, A.J. Levine, Surfing the p53 network, Nature 408 (2000) 307–310.
[5] K.W. Kinzler, B. Vogelstein, Life (and death) in a malignant tumor, Nature 379 (1996) 19–20.
[6] W.S. El-Deiry, T. Tokino, V.E. Velculescu, et al., WAF-1, a potential mediator of p53 tumor suppression, Cell 75 (1993) 817–825.
[7] W.S. El-Deiry, Regulation of p53 downstream genes, Sem. Cancer Biol. 8 (1998) 345–357.
[8] T. Tokino, S. Thiagalingam, W.S. El-Deiry, T. Wladman, K.W. Kinzler, B. Vogelstein, p53 tagged sites from human genomic DNA, Hum. Mol. Genet. 3 (1994) 1537–1542.
[9] W.S. El-Deiry, S.E. Kern, J.A. Pietenpol, K.W. Kinzler, B. Vogelstein, Definition of a consensus binding site for p53, Nat. Genet. 1 (1992) 45–49.
[10] X. Wu, H. Bayle, D. Olson, A.J. Levine, The p53-mdm2 autoregulatory feedback loop, Genes Dev. 7 (1993) 1126–1132.
[11] A. Zauberman, D. Flusberg, Y. Haupt, Y. Barak, M. Oren, A functional p53-responsive intronic promoter is contained within the human mdm2 gene, Nucl. Acids Res. 23 (1995) 2584–2592.
[12] S.E. Kern, K.W. Kinzler, A. Bruskin, et al., Identification of p53 as a sequence specific DNA-binding protein, Science 252 (1991) 1708–1711.
[13] M. Hollstein, M. Hergenhahn, Q. Yang, H. Bartsch, Z.Q. Wang, P. Hainaut, New approaches to understanding p53 gene tumor mutation spectra, Mutat. Res. 431 (1999) 199–209.
[14] Y. Cho, S. Gorina, P.D. Jeffrey, N.P. Pavletich, Crystal structure of a p53 tumor suppressor–DNA complex: understanding tumorigenic mutations, Science 265 (1994) 346–355.
[15] P.N. Friedman, X. Chen, J. Bargonetti, C. Prives, The p53 protein is an unusually shaped tetramer that binds directly to DNA, Proc. Natl. Acad. Sci. USA 90 (1993) 3319–3323.
[16] P. Balagurumoorthy, H. Sakamoto, M.S. Lewis, et al., Four p53 DNA-binding domain peptides bind natural p53-response elements and bend the DNA, Proc. Natl. Acad. Sci. USA 92 (1995) 8591–8595.
[17] A.K. Nagaich, V.B. Zhurkin, H. Sakamoto, et al., Architectural accommodation in the complex of four p53 DNA binding domain peptides with *p21/waf1/cip1* DNA response-element, J. Biol. Chem. 272 (1997) 14830–14841.
[18] D.I. Cherny, G. Striker, V. Subramanian, S.D. Jett, E. Palecek, T.M. Jovin, DNA bending due to specific p53 and p53 core domain–DNA interactions visualized by electron microscopy, J. Mol. Biol. 294 (1999) 1015–1026.
[19] A.K. Nagaich, V.B. Zhurkin, S.R. Durell, R.L. Jernigan, E. Appella, R.E. Harrington, p53 induced DNA bending and twisting: p53 tetramer binds on the outer side of a DNA loop and increases DNA twisting, Proc. Natl. Acad. Sci. USA 96 (1999) 1875–1880.
[20] S.R. Durell, E. Appella, A.K. Nagaich, R.E. Harrington, R.L. Jernigan, V.B. Zhrukin, DNA bending induced by tetrameric binding of the tumor-suppressor p53 protein: steric constraints on conformation, in: R.H. Sarma, M.H. Sarma (Eds.), Structure, Motion, Interaction and Expression of Biological Macromolecules. Proceedings of the Tenth Conversation, Adenine Press, Schenectady, NY, 1998, pp. 277–295.
[21] H. Zhou, Y. Zhang, Z.-C. Ou-Yang, et al., Conformation and rigidity of DNA microcircles containing waf1 response element for p53 regulatory protein, J. Mol. Biol. 306 (2001) 227–238.
[22] A.K. Nagaich, E. Appella, R.E. Harrington, DNA bending is essential for the site-specific recognition of DNA response elements by the DNA binding domain of the tumor suppressor protein p53, J. Biol. Chem. 272 (1997) 14842–14849.
[23] Z. Miner, M. Kulesz-Martin, DNA binding specificity of proteins derived from alternatively spliced mouse p53 mRNAs, Nucl. Acids Res. 25 (1997) 1319–1326.
[24] J.L.F. Waterman, J.L. Shenk, T.D. Halazonetis, The dihedral symmetry of the p53 tetramerization domain mandates a conformational switch upon DNA binding, EMBO J. 14 (1995) 512–519.
[25] V.B. Zhurkin, Y. Lysov, V.I. Ivanov, Anisotropic flexibility of DNA and the nucleosome structure, Nucl. Acids Res. 6 (1979) 1081–1096.
[26] W.K. Olson, A.A. Gorin, X.-J. Lu, L.M. Hock, V.B. Zhurkin, DNA sequence dependent deformability

deduced from protein–DNA crystal complexes, Proc. Natl. Acad. Sci. USA 95 (1998) 11163–11168.
[27] W.K. Olson, V.B. Zhurkin, Modeling DNA deformations, Curr. Opin. Struct. Biol. 10 (2000) 286–297.
[28] P.T. McNamara, A. Bolshoy, E.N. Trifonov, R.E. Harrington, Sequence dependent kinks induced in curved DNA, J. Biomol. Struct. Dyn. 8 (1990) 529–538.
[29] T.A. Steitz, Structural studies of protein–nucleic acid interaction: the sources of sequence specific binding, Q. Rev. Biophys. 23 (1990) 205–280.
[30] S.C. Schultz, C.C. Shields, T.A. Steitz, Crystal structure of a CAP–DNA complex: the DNA is bent by 90°, Science 253 (1991) 1001–1007.
[31] Y.L. Lyubchenko, L.S. Shlyakhtenko, B. Chernov, R.E. Harrington, DNA bending induced by cro protein binding as demonstrated by gel electrophoresis, Proc. Natl. Acad. Sci. USA 88 (1991) 5331–5334.
[32] R.E. Harrington, DNA curving and bending in protein-DNA recognition, Mol. Microbiol. 6 (1992) 2549–2555.
[33] R.E. Harrington, Studies of DNA bending and flexibility using gel electrophoresis, Electrophoresis 14 (1993) 732–746.
[34] M.A. ElHassan, C.R. Calladine, Structural mechanics of bent DNA, Endeavor 20 (1996) 61–67.
[35] C.M. Nunn, S. Neidle, The high resolution crystal structure of the DNA decamer d(AGGCATGCCT), J. Mol. Biol. 256 (1996) 340–351.
[36] L. Ulanovsky, M. Bodner, E.N. Trifonov, M. Choder, Curved DNA: design, synthesis and circularization, Proc. Natl. Acad. Sci. USA 83 (1986) 862–866.
[37] R.G. Brennan, S.L. Roderick, Y. Takeda, B.W. Matthews, Protein–DNA conformational changes in the crystal structure of a λ cro-operator complex, Proc. Natl. Acad. Sci. USA 87 (1990) 8165–8169.
[38] D.A. Erie, G.L. Yang, H.C. Schultz, C. Bustamante, DNA bending by cro protein in specific and non-specific complexes: implications for protein site recognition and specificity, Science 266 (1994) 1562–1566.
[39] R.E. Harrington, I. Winicov, in: W. Cohn, K. Moldave (Eds.), Progress in Nucleic Acids Research and Molecular Biology, 47, Academic Press, San Diego, 1994, pp. 195–270.
[40] W.H. Han, S.M. Lindsay, T. Jing, A magnetically driven oscillating probe microscope for operation in liquids, Appl. Phys. Lett. 69 (1996) 4111–4114.
[41] W.H. Han, M. Dlakic, Y.W. Zhu, S.M. Lindsay, R.E. Harrington, Strained DNA is kinked by low concentrations of Zn^{2+}, Proc. Natl. Acad. Sci. USA 94 (1997) 10565–10570.
[42] Y.L. Lyubchenko, R.E. Blankenship, A.A. Gall, et al., Atomic force microscopy of DNA, nucleoproteins and cellular complexes: the use of functionalized substrates, Scanning Microsc. Suppl. 10 (1996) 97–107.
[43] J.M. Espinosa, B.M. Emerson, Transcriptional regulation by p53 through intrinsic DNA/chromatin binding and site-directed cofactor recruitment, Mol. Cell 8 (2001) 57–69.
[44] P. Sudarsanam, Y. Cao, L. Wu, B.C. Laurent, F. Winston, The nucleosome remodeling complex, Snf/Swi, is required for the maintenance of transcription in vivo and is partially redundant with the histone acetyltransferase, Gen5, EMBO J. 18 (1999) 3101–3106.
[45] I. Gavin, P.J. Horn, C.L. Peterson, SWI/SNF chromatin remodeling requires changes in DNA topology, Mol. Cell 7 (2001) 97–104.
[46] C.J. Fry, C.L. Peterson, Chromatin remodeling enzymes: who's on first?, Curr. Biol. 11 (2001) R185–197.
[47] M. Lorenz, A. Hillisch, D. Payet, M. Buttinelli, A. Travers, S. Diekmann, DNA bending induced by high mobility group proteins studied by fluorescence resonance energy transfer, Biochemistry 38 (1999) 12150–12158.
[48] V. Aidinis, T. Bonaldi, M. Beltrame, S. Santagata, M.E. Bianchi, E. Spanopoulou, The RAG1 homeodomain recruits HMG1 and HMG2 to facilitate recombination signal sequence binding and to enhance the intrinsic DNA-bending activity of RAG1–RAG2, Mol. Cell. Biol. 19 (1999) 6532–6542.
[49] L. Tang, J. Li, D.S. Katz, J.A. Feng, Determining the DNA bending angle induced by non-specific high mobility group-1 (HMG-1) proteins: a novel method, Biochemistry 39 (2000) 3052–3060.
[50] L. Jayaraman, N.C. Moorthy, K.G. Moorthy, J.L. Manley, M. Bustin, C. Prives, High mobility group protein-1 (HMG-1) is a unique activator of p53, Genes Dev. 12 (1998) 462–472.